Supervirtual S-wave refraction interferometry for converted wave statics and near-surface S-wave velocity model building

Kristof De Meersman[(1)] and Yoones Vaezi[(1,2)]
CGG[1], University of Alberta[2]

Summary

Lack of knowledge of near-surface S-wave velocities is one of the principal issues when processing converted wave data. Many land multi-component datasets do, however, contain S-wave refraction arrivals which, if picked, could provide this information. These refracted S-wave arrivals are rarely used because they are difficult to identify, not the first arrival and of general low signal-to-noise. Supervirtual refraction interferometry is a new technique that can dramatically improve the signal-to-noise ratio of noisy P-wave refractions in supervirtual gathers. We have tested this method on S-wave refractions from a 2D 3C dataset. Accurate first break S-wave arrivals could be picked on the supervirtual gathers and were subsequently inverted for a near-surface S-wave velocity structure which can be used to calculate PS receiver statics. We demonstrate the usefulness of this method for converted-wave imaging and near-surface S-wave velocity model building by analyzing the computed receiver statics on PS images and gathers.

Introduction

One fundamental problem when imaging converted-wave (PS) data is our lack of knowledge of the near-surface S-wave velocity structure. This makes it difficult to derive receiver statics for time imaging and severely affects our ability to depth migrate. Moreover, near-surface S-wave velocities are often unrelated (uncorrelated) to P-wave velocities. In the absence of near-surface S-wave velocity information most PS statics methods rely on interpretation, such as matching the PS structure to PP structure on receiver stacks. This is often problematic as it is difficult to obtain a good quality structural image in early PS processing, especially when the statics are unknown. Residual statics methods are also popular but often fail to provide a robust long-wavelength solution and are prone to cycle skipping due to the very large time shifts.

One method that has been proposed to obtain near-surface S-wave velocities is surface or Rayleigh-wave dispersion curve inversion. For the purpose of deriving PS-wave receiver statics, however, there are relatively few documented successful case histories (Haney and Douma, 2012). Alternatively, others have proposed S-wave first break picking and inversion to solve the PS statics problem (Bansal et al., 2009, Schafer 1991). Conventional (vertical) vibroseis and explosive sources are excellent S-wave generators (White, 1983; Lee & Balch, 1982), which are emitted at high take-off angles making them ideally suited for refraction and turning wave analysis. However, S-wave refractions are rarely used because they are difficult to pick. The most obvious reason for this is that they are not the first arrival on radial component gathers and suffer from low signal-to-noise ratio due to interference from converted-wave energy and ambient noise. They are also typically of much lower bandwidth compared to P-wave first breaks and may be spatially aliased.

In the following we use "supervirtual refraction interferometry" (SVI) to boost the signal-to-noise ratio of S-wave refractions on radial component (PS) gathers. SVI is a fairly new method that has been applied to P-wave refractions with promising results (Mallinson et al., 2011). We have implemented the SVI method on S-wave refractions from a 2D-3C survey in Alberta, Canada. The resulting supervirtual refraction gathers were used to pick accurate S-wave first breaks. Turning ray tomography (Zhu et al., 2000) was then used to invert these picks for near-surface S-wave velocities. The resulting statics agree well with those obtained by conventional PP-PS horizon matching and multiple passes of residual statics.

Theory of supervirtual refraction interferometry

Here we provide a short review of the supervirtual refraction interferometry (SVI) theory. A more complete theoretical description of SVI can be found in (Bharadwaj et al., 2012). SVI was originally developed for P-wave head waves but applies equally to S-wave refractions. Assume the 2D geometry shown in Figure 1. The refractor interface can have any smooth topography.

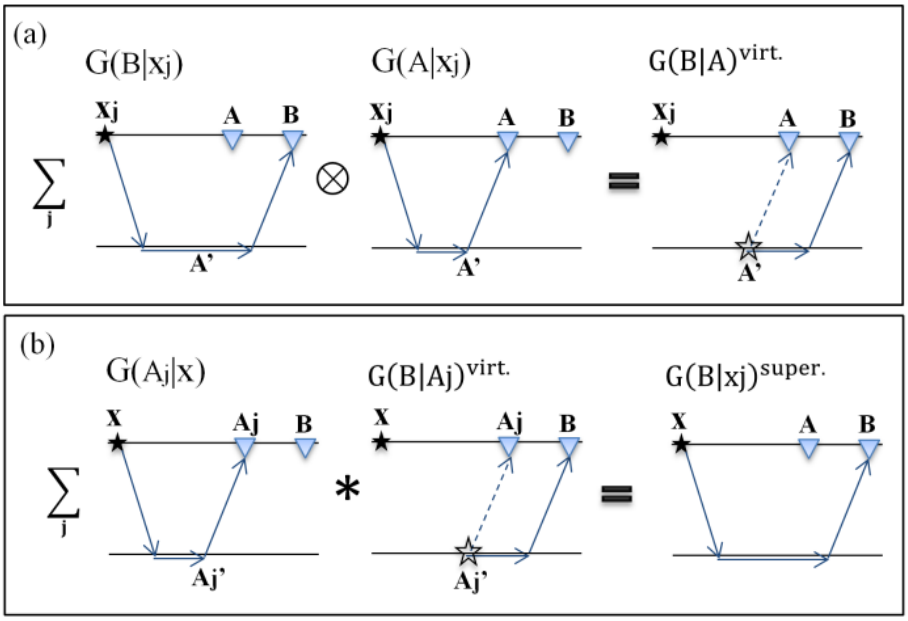

Figure 1*. Supervirtual refraction Interferometry consists of two main steps. (a) The first step is the cross correlation of data from any two receivers* ***A*** *and* ***B*** *for all post-critical sources* x_i*. These are summed to form virtual refractions* $G(B|A)^{virt}$*. (b) The second step is the convolution of recorded data from source X and receiver* A_i *with a virtual trace between receivers* A_i *and B. This is repeated for all receivers* A_j *and the results summed to give the supervirtual refractions* $G(B|xj)^{super}$*.*

The head-wave arrivals emitted by a source at xj and recorded by receivers at A and B are denoted by G(A|x) and G(B|x), respectively, where G is the Green's function. The SVI technique consists of two main steps. The first step (Figure 1a) is the cross correlation of records from receivers A and B for every post critical source xj and then summing over all these sources,

$$Im\left[G(B|A)^{virt}\right] \approx k \sum_{j=1}^{N_s} G(B|x_j)G(A|x_j)^* \qquad (1)$$

where k is the average wavenumber at the receivers, and N_S is the number of post-critical sources for receiver **B**. The asterisk (*) denotes complex conjugation, and *Im*[*G*] represents the imaginary part of *G*. The common ray paths cancel in the cross correlation resulting in a virtual head wave that would have been emitted by a virtual source located at sub-surface location **A'** and recorded at **B**. It has a negative excitation time corresponding to the travel time

between **A** and **A'**. The second step (Figure 1b) consists of convolving a shot gather from source ***x*** with previously computed virtual refractions between receivers $\boldsymbol{A_i}$ and ***B***. Receiver ***B*** is located at an offset greater than $\boldsymbol{A_i}$ and the resulting convolutions are summed over N_r post-critical intermediate receivers $\boldsymbol{A_j}$ to give a 'supervirtual trace' at receiver ***B***:

$$G(B|x)^{super} \approx 2ik \sum_{j=1}^{N_r} G(A_j|x)G(B|A_j)^{virt.} \quad (2)$$

Supervirtual traces $G(B|x)^{super}$ have the same source and receiver locations as the original recorded data $G(B|x)$ and the same kinematics of the S-wave refraction, but with an enhanced S/N that results from the stacking in SVI. The further a receiver is from the source the more intermediate receivers A_j can be involved in the stacking step and the greater the potential S/N increase. According to the general theory of SVI the S/N ratio of far-offset head-wave arrivals can increase by a factor proportional to $\sqrt{N_r}$, where N_r is the number of intermediate offset and post critical receivers included (Bharadwaj et al., 2012).

Analysis and results

For our experiment we used radial component data from a 2D 3C line acquired by the CREWES consortium in Hussar, Alberta, Canada (Margrave et al., 2012). Our test dataset used a total of 269, 15 m deep explosive sources at 20 m interval and 248 3C 10 Hz geophones placed at a 10 m interval. Figure 2a shows a typical common shot gather after applying a 1000 ms AGC and a 20-40 Hz low-pass filter. The S-wave refraction is identified using yellow arrows. Contrary to P-wave refractions it is clearly not the first arrival on a seismic gather. This S-wave refraction suffers from interference by converted-wave energy (PS reflections) as well as significant amounts of coherent secondary source noise which is probably caused by generators.

Prior to running the SVI workflow the raw data is pre-conditioned by low-pass filtering (10-15 Hz), AGC and windowing around the S-wave direct arrival, Figure 2b. Pre-critical traces (<100 m offset) are also discarded as they do not contribute in the generation of the virtual traces. This pre-conditioning isolates the portion of the data with best S/N for the refracted S-wave and reduces the influence of interfering seismic energy in the cross correlation (Dong et al., 2006). The corresponding supervirtual gather is shown in Figure 2c. The effects of coherent noise have been reduced dramatically compared to the original preconditioned data. Also at an offset of 2500 m the supervirtual data appear to have recovered moveout features that are possibly related to near surface statics and which were not visible on the raw data due to poor S/N. The supervirtual gathers are, however, very band limited with many side lobes, mostly due to the harsh preconditioning.

The supervirtual gathers are then used to perform S-wave first break picking and the picks inverted for near-surface S-wave velocities using a turning ray tomography. In order to overcome picking problems due to the many side lobes we used the raw data to seed a few picks onto the supervirtual gathers and guide the automatic picking along a consistent phase. These picks are shown as green curves on Figures 2b and 2c. The blue curves in Figures 2b and 2c show the predicted S-wave first-breaks by the tomographic inversion. They are in good agreement with the data, indicating a good convergence of the tomography. Figures 2d and 2e show fully processed radial component shot gathers before and after applying the PS receiver statics that were calculated from our supervirtual S-wave first breaks. Likewise, fully processed PS receiver stacks without any receiver statics and with our receiver statics solution are shown in Figures 2f and 2g. In comparison, Figure 2h shows a PS receiver stack with a conventional receiver statics solution that is obtained by PP-PS structural matching and multiple passes of

residual and hand statics. The near-surface tomographic S-wave velocity model has clearly resolved the PS receiver static. Some residual and short wavelength receiver statics remain (black arrow in Figure 2g). This is not uncommon for turning ray tomography statics solutions as some spatial smoothing of the velocity model is often required for stability. A single pass of residual statics is expected to resolve this and lead to a final solution that is comparable in quality to a 'conventional' and labor intensive PS receiver statics solution. Moreover, The SVI weathering statics solution can be obtained prior to velocity analysis and is thus independent of the quality of the initial imaging.

Conclusions

Most conventional seismic sources on land are favourable for generating vertically polarized S-wave refractions. These S-wave refractions are present on most 3C datasets on the radial component. They are however not the first arrival, of fairly low bandwidth, typically of very poor signal-to-noise and difficult to identify and/or pick. We have successfully tested 2D supervirtual refraction interferometry on the radial component of a Canadian 2D 3C dataset. This has improved the quality of the S-wave first arrival sufficiently to allow picking and subsequent tomographic inversion. The resulting near-surface S-wave velocity model was used to compute converted-wave receiver statics. Analysis of these statics on gathers and stacks indicate that they successfully correct for near-surface S-wave velocity variations.

Acknowledgements

The authors would like to express their gratitude towards CREWES for acquiring the data and providing show rights and to CGG for supporting this research and permitting publication. Many thanks to members of the CGG multicomponent research team for their continuous feedback on the project. We also thank Monica Deviat for the original processing and Martin Fuhrer, Alice Chapman, Terence Krishnasamy, Harry Du, Lisbeth Velasquez, and Art McCarthy for their assistance.

References

Bansal, R., Ross, W., Lee, S., Matheney, M., Martinez, A., Jenkinson, T., and Shatilo, A. [2009] A novel approach to estimating near-surface S-wave velocity and converted-wave receiver statics, *SEG Technical Program Expanded Abstracts*. doi: 10.1190/1.3255065.

Bharadwaj, P., Schuster, G., Mallinson, I. and Dai, W. [2012] Theory of supervirtual refraction interferometry, *Geophys. J. Int*., **188**, 263–273.

Dong, S., Sheng, J. and Schuster, G. [2006] Theory and practice of refraction interferometry, *SEG Expand. Abstr.,* **25**, 3021–3025.

Haney M. and Douma H. [2012] Rayleigh wave tomography at Coronation Field, Canada: The topography effect, The Leading Edge, 31, p.54-61,

Lee, M. W. and A. H. Balch, 1982. Theoretical seismic wave radiation from a fluid -filled borehole: Geophysics, 47, 1308-1314

Mallinson, I., Bharadwaj, P., Schuster, G. and Jakubowicz, H. [2011] Enhanced refractor imaging by super-virtual interferometry, *The Leading Edge*, **30**, 546–550.

Margrave, G. F., Mewhort, L., Phillips, T., Hall, M., Bertram, M. B., Lawton, D. C., Innanen, K., Hall, K. W., and Bertram, K. [2012] The Hussar low-frequency experiment, CSEG Recorder, Vol. 37, No. 7, 25-39.

Schafer, A. [1991] Determination of converted-wave statics using P refractions together with SV refractions. SEG Technical Program Expanded Abstracts: pp. 1413-1415. doi: 10.1190/1.1889086.

White, J. E. [1983] Underground sound – Applications of seismic waves: Elsevier Science Publishers.

Zhu, T., Cheadle, S., Petrella, A., and Gray, S. [2000] First-arrival tomography: Method and application, 70th Annual international Mtg., Soc. Expl. Geophys., Expanded Abstracts, 2028-2031.

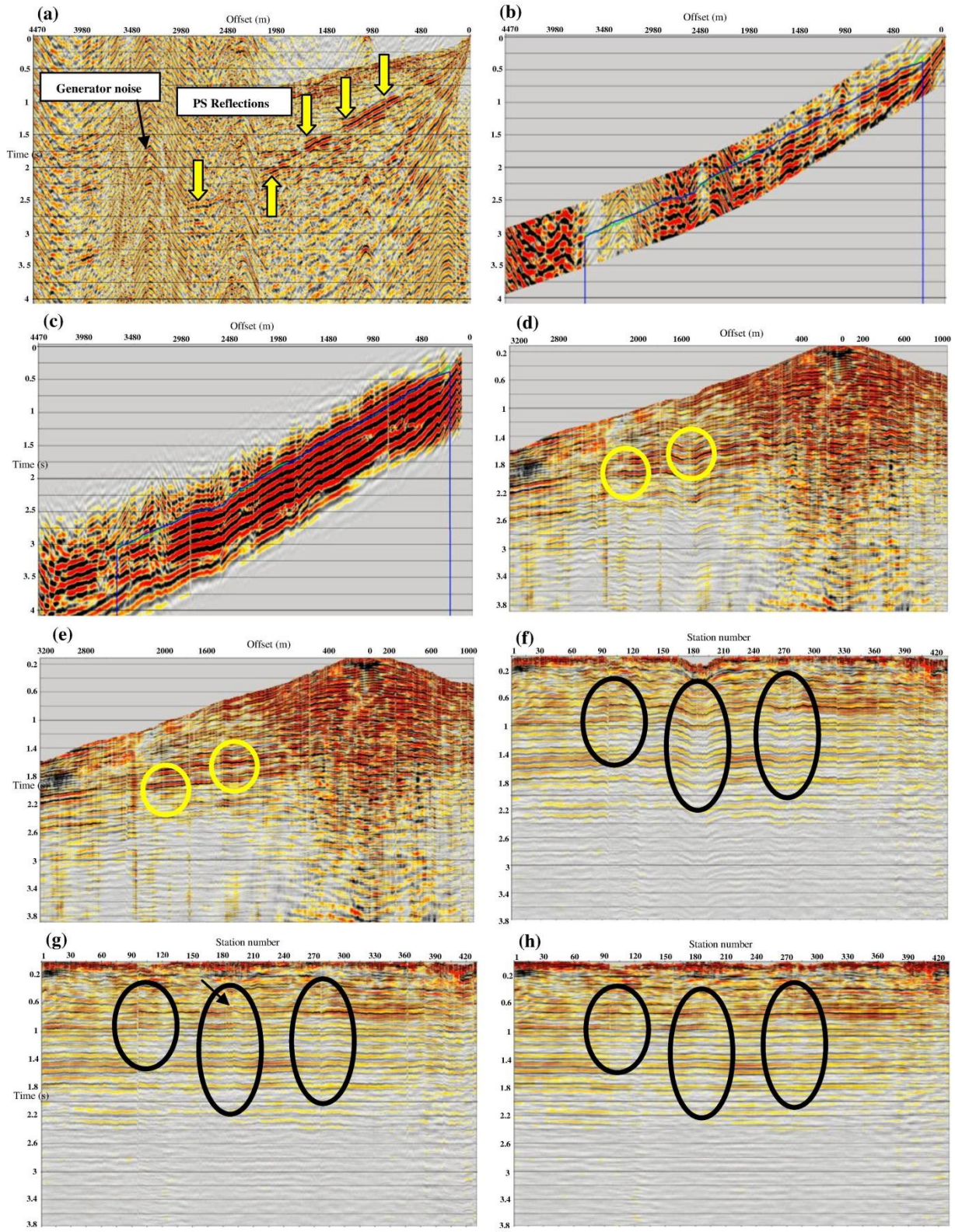

***Figure 2**. (a) Shot after AGC and a 20-40 Hz low-pass filter (b) The same gather with a 5-10 Hz low-pass filter and windowed around the S-wave first arrivals. The curves show the picked (green) and the calculated (blue) FB picks. (c) The corresponding supervirtual gather. (d) & (e) A shot gather before and after removing the S-wave weathering statics calculated from SVI FB picks. (f) & (g) Receiver stacks before and after removing the SVI weathering statics. (h) The final receiver stack obtained by 'conventional C-wave processing' which includes PP-PS structural matching and 4 passes of residual statics.*